ELSEVIER

Journal of Power Sources 105 (2002) 26–34

JOURNAL OF POWER SOURCES

www.elsevier.com/locate/jpowsour

Ethanol reforming for hydrogen production in a hybrid electric vehicle: process optimisation

V. Klouz[a], V. Fierro[a], P. Denton[a], H. Katz[b], J.P. Lisse[b], S. Bouvot-Mauduit[c], C. Mirodatos[a,*]

[a]*Institut de Recherches sur la Catalyse, CNRS, 69626 Villeurbanne, France*
[b]*Peugeot Citroën, Direction de la Recherche et de l'Innovation Automobile, 78140 Vélizy, France*
[c]*Agence de l'Environnement et de la Maîtrise de l'Energie, 75737 Paris, France*

Received 20 May 2001; received in revised form 1 September 2001; accepted 18 September 2001

Abstract

This work is focused at optimizing an ethanol reforming process over a Ni/Cu catalyst to produce a hydrogen rich stream in order to feed a solid polymer fuel cell (SPFC). The effect of the reaction temperature, H_2O/EtOH and O_2/EtOH molar ratios of the feed to the reformer was studied under diluted conditions in order to maximize the hydrogen content and the CO_2/CO_x molar ratio at the outlet of the ethanol reformer. Based on the experimental results, a detailed kinetic scheme of the ethanol reforming was discussed as a function of the temperature, special attention was paid to the role of oxygen in the reaction selectivity and coke formation. Moreover, the coke nature was evaluated by transmission electron microscopy (TEM) and TPO and TPH experiments. The tests carried out at on-board reformer conditions allowed a hydrogen rich mixture (33%) in the outlet reformer flow that can be even increased by water gas sift reactions downstream. The high hydrogen content of the flow to the fuel cell together with the stability of the Ni/Cu catalyst, fully demonstrated by long time runs, can be considered of high interest for SPFC applications.

Keywords: Solid polymer fuel cell; Ethanol steam reforming; Hybrid car

1. Introduction

The development of electric vehicles, offering zero emission of pollutants, constitutes a priority objective to limit urban pollution [1,2]. The storage of electricity in batteries presents not yet resolved technological issues. This is why the chemical storage of energy is currently preferred. The fast development of fuel cell technologies [3] and particularly of solid polymer fuel cell (SPFC) [4], involves the storage of a liquid fuel free from sulfur and metals, which would be easily transformable into hydrogen without polluting emissions.

Alcohols exhibit high qualities as H_2 generators, since they are easily decomposed in the presence of water (steam reforming reaction) and generate a H_2-rich mixture suitable for feeding fuel cells, provided that carbon monoxide is further on oxidised into carbon dioxide. As a matter of fact, usual SPFCs require to be fed with hydrogen containing less than 10 ppm CO.

The methanol steam reforming has been thoroughly studied in recent years, since methanol is available as an abundant feedstock and already largely distributed. Methanol also presents a favorable H/C ratio. Complete on-board H_2-generation systems from methanol have been described [5,6]. Prototypes have even been exhibited by Toyota [7] and Daimler Chrysler [8]. However, the main drawback of methanol, beside its relatively high toxicity, is that its production is essentially based on reforming of non-renewable fossil fuels (mostly natural gas), and therefore its use as a feedstock for electrical vehicle will release fossil carbon into the atmosphere.

Ethanol appears as an attractive alternative to methanol, since it is much less toxic [9], and is already used as versatile transportation fuel that offers a high octane number, a high heat of vaporisation and a low photochemical reactivity. Moreover, bio-ethanol can be produced in large quantities from biomass fermentation therefore, as a renewable energy source. This alcohol has also a significant advantage over fossil fuel based systems: it is CO_2 neutral, since the carbon dioxide that is produced in the process is consumed by biomass growth and a closed carbon cycle is operated. Thus, ethanol appears as one of the best candidates provided that its steam reforming can induce a controlled production of hydrogen which accommodates the electric car requirements. Few studies about ethanol steam reforming have been

* Corresponding author. Tel.: +33-472-44-5366; fax: +33-472-44-5399.
E-mail address: mirodato@catalyse.univ-lyon1.fr (C. Mirodatos).

0378-7753/02/$ – see front matter
PII: S0378-7753(01)00922-3

published up to now, dealing either with the thermodynamic analysis of the water /ethanol system [10–14] or with preliminary catalytic testing experiments [15–23].

The catalytic properties of supported transition metal catalysts for ethanol reforming, especially cobalt, and the effect of the particle size and the nature of the support were investigated by Haga et al. [19–22]. Although they concluded that selectivity for the reaction was in the order Co > Ni > Rh > Pt, Ru, Cu, most of the catalysts investigated for the reforming of ethanol are Ni-based catalysts with additions of Cu, Cr, Zn or K [16–18,23]. It is generally accepted that nickel promotes C–C bond rupture whereas the role played by the additives is still under discussion. Luengo et al. [16] suggested that Cu and Cr are responsible for the subsequent oxidation of methanol into CO and H_2 whereas Mariño et al. [23] concluded that Cu is the active agent.

In a recent work, Freni [24] has studied the reforming of a water/ethanol mixture on a Rh based catalyst as an alternative fuel for molten carbonate fuel. Despite the high H_2 concentration (about 30% at 650 °C) in the outlet gases the cost of this catalyst appears to be the main drawback.

Concerning the operating temperature and H_2O/EtOH ratio, Fishtik et al. [13] carried out a thermodynamic analysis of hydrogen production from ethanol steam reforming. They found that for temperatures at or above 400–500 °C and for high water/ethanol ratios the desired reaction of ethanol steam reforming is predominant and the amount of undesired products, CO and CH_4, is minimized. A more recent thermodynamic analysis by Ioannides [14] has concluded that a H_2O/EtOH molar ratio higher than stoichometry results in reduced efficiency in hydrogen production, because of increased enthalpy needs for water evaporation. When air is co-fed with ethanol, optimal operating conditions can be found as a function of the preheat temperature of the feed.

This paper presents, the optimisation of the ethanol steam reforming as part of an on-board integrated H_2 generator system. Accordingly, the optimisation criteria are directly related to the proposed process (internal reforming supplying a SPFC). After an initial step of active and selective catalyst selection for ethanol reforming, the different experimental parameters such as temperature, H_2O/EtOH molar ratio, introduction of oxygen in the feed gas and contact time, are studied and optimised outside the car utilisation constraints. A further study (not reported here) has been carried out under conditions closer to the on-board ones and the results patented [25].

2. Experimental

2.1. Catalyst

The active and selective material selected for ethanol steam reforming is a Ni-Cu/SiO_2 [25] catalyst prepared by impregnating a silica support (Degussa) with a BET surface of 200 $m^2\,g^{-1}$ and by using $Ni(NO_3)_2{\cdot}6H_2O$ and $Cu(NO_3)_2{\cdot}3H_2O$ as precursors. The catalyst has a Cu/(Ni + Cu) weight ratio of 10 and a total metal content of 18.4%. After calcination at 400 °C for 15 h, the catalyst is sieved to 0.2 and 0.3 mm.

2.2. Catalytic tests

Prior to catalytic testing, the catalyst was placed in a fixed bed reactor and reduced under flowing hydrogen (30 ml min^{-1}) at 650 °C for 8 h with a heating rate of 2 °C min^{-1}. After reduction the catalyst is cooled down to reaction temperature. The runs were performed under diluted conditions with helium as diluent (94% He) at atmospheric pressure in a fixed bed reactor (ID = 4 and H_{bed} = 7 mm), where 15–50 mg of the catalyst are introduced. Catalyst was dispersed with SiC to minimize hot spot effects.

A saturator-condenser kept at 18 °C is used to saturate the inert gas flow with ethanol ensuring a partial pressure of 5085 Pa. Water is synthesised in situ, with helium as diluent and Pt/Al_2O_3 (Aldrich) as catalyst. The total flow rate is maintained at 50 ml min^{-1}. The reactants and the products in the effluent gases are analysed by gas chromatography (Carbosieve column—thermal conductivity detector and HayeSep D column—flame ionisation detector). Additional gas analyses are performed by on-line mass spectrometry (VG Quadrupole).

2.3. Kinetic parameter formulae

The reactants conversion (ethanol, water or oxygen), denoted $X_{reactant}$, and the products selectivity (hydrogen, methane, carbon oxides, acetaldehyde), denoted $S_{product}$, are calculated according to Eqs. (1) and (2), respectively. $F_{i,\,\text{in or out}}$ represents the molar flow rate of the i species measured at the inlet or at the outlet of the reactor and n is the stoichiometric factor between the carbon-containing products and ethanol. The amount of carbon deposited per hour and per gram of catalyst is given by Eq. (4). When water is a reaction product, its selectivity is determined in relation to ethanol (Eq. (5)). Since this work was carried out at diluted conditions (94% He) a correction factor accounting for the volume change due to reaction was not considered to calculate conversions and selectivities.

$$X_{\text{reactant}} = \frac{F_{\text{reactant in}} - F_{\text{reactant out}}}{F_{\text{reactant in}}} \tag{1}$$

$$S_{H_2} = \frac{F_{H_2\,\text{produced}}}{F_{H_2\,\text{consumed}}} = \frac{F_{H_2}}{[3(F_{\text{EtOH in}} - F_{\text{EtOH out}}) + (F_{H_2O\,\text{in}} - F_{H_2O\,\text{out}})]} \tag{2}$$

$$S_{\text{carbon-containing product}} = \frac{F_{\text{carbon-containing product}}}{(F_{\text{EtOH in}} - F_{\text{EtOH out}})n} \tag{3}$$

$$C_{\text{deposited}} = \frac{(F_{\text{carbon in}} - F_{\text{carbon out}})12}{m_{\text{catalyst}}} \quad (4)$$

$$S_{H_2O} = \frac{F_{H_2O}}{3(F_{\text{EtOH in}} - F_{\text{EtOH out}})} \quad (5)$$

$$t_c = \frac{m_{\text{cata}}\,(\text{kg})}{\text{EtOH}\,(\text{mol min}^{-1})} \quad (6)$$

$$\frac{CO_2}{CO_x} = \frac{F_{CO_2\,\text{out}}}{(F_{CO_2\,\text{out}} + F_{CO\,\text{out}})} = \frac{S_{CO_2}}{S_{CO_2} + S_{CO}} \quad (7)$$

The contact time, denoted t_c in Eq. (6), is defined as the ratio between the mass of catalyst and the molar flow of the inlet ethanol. Though contact time is usually defined as the ratio between the mass of catalyst and the total inlet flow rate, the present definition focuses on the ethanol contact time for a direct evaluation of the link between the active sites concentration and the number of ethanol moles to convert.

2.4. Characterization of carbon deposits

Carbon deposits accumulated on the catalyst during ethanol steam reforming runs for a given time on stream are analysed by temperature programmed oxidation (TPO) or by temperature programmed hydrogenation (TPH). After being cooled to room temperature under inert atmosphere, the used catalyst is heated at linearly increasing tempera–ture (10 °C min^{-1}), up to 900 °C either under oxygen (20 vol.% in He) or hydrogen (5 vol.% in He). The formation of carbon dioxide for TPO and of methane for TPH is followed by on-line mass spectrometry. The amount of carbon deposited on the aged catalysts can be determined from the integration of the CO_2 (TPO) or CH_4 (TPH) production curves as a function of time/temperature.

Additional characterization of carbon deposits was performed by high resolution transmission electron microscopy (TEM) on a JEOL 2010 microscope.

3. Results

3.1. Influence of the temperature

Fig. 1 illustrates the effect of temperature on reactants conversion and products selectivity. According to the stoichiometry of the global steam reforming reaction ($C_2H_5OH + 3H_2O = 6H_2 + 2CO_2$), the molar ratio H_2O/EtOH is initially fixed to 3.7 in order to have an excess of water.

Unless ethanol that is completely converted over the whole studied temperature range, the conversion of water increases with temperature. The negative value obtained at 300 °C indicates that more water is formed than consumed ($X_{H_2O} = [F_{H_2O\,\text{in}} - F_{H_2O\,\text{out}}]/F_{H_2O\,\text{in}} < 0 \Rightarrow F_{H_2O\,\text{in}} < F_{H_2O\,\text{out}}$). In this case, the selectivity to hydrogen is calculated with respect to the consumed ethanol.

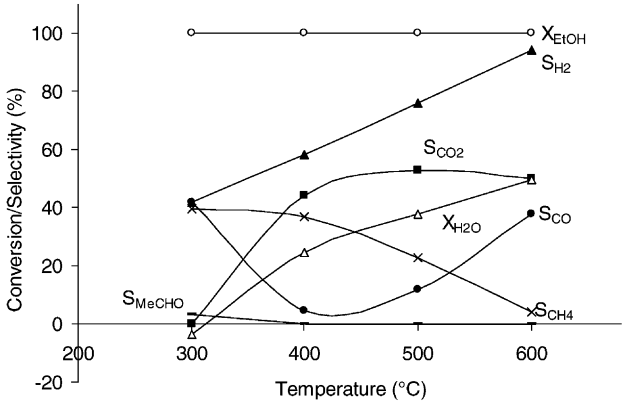

Fig. 1. Conversion of ethanol and water and product selectivity vs. temperature (H_2O/EtOH = 3.7, O_2/EtOH = 0 and t_c = 0.9 min kg mol^{-1}).

Except at 300 °C where acetaldehyde is observed as a product of ethanol oxidation, methane is the only by-product of the reforming reaction to syngas from 400 to 600 °C. The selectivity to H_2 and CO increases with temperature, whereas the selectivity to CH_4 decreases. The selectivity to CO_2, almost negligible at 300 °C, increases up to 500 °C and decreases at 600 °C.

From the above results, the best selectivity to hydrogen is obtained at 600 °C, so this temperature will be considered for testing other operating parameters aiming at keeping the CO_2/CO_x ratio high enough for the downstream processes of the on-board system.

3.2. Characterisation of the carbon deposition

During the previous test the carbon mass balance ($S_{CO} + S_{CO_2} + S_{CH_4} + S_{MeCHO}$) stays below 100%, indicating carbon deposition. TPO experiments show that most of the deposited carbon can be oxidised into CO_2 (no water formation) at relatively high temperature (maximum of CO_2 production at 580 °C) and its amount is found little dependent on the reforming temperature (around 130 mg h^{-1} $\text{g}_{\text{cat}}^{-1}$).

TPH experiments carried out after similar reforming runs reveal that two types of carbon are deposited during ethanol reforming (Fig. 2): (i) a highly reactive carbon, denoted C_{LT}, which is hydrogenated into methane at low temperature (200 °C) but in a small amount (7 μg after 25 min and 13 μg after 1 h 50 min of reforming reaction); and (ii) a less reactive carbon, denoted C_{HT}, which is hydrogenated at higher temperatures (maximum at 620 °C) but represents about 96% of the total amount of the hydrogenated carbon (0.17 mg after 25 min and 0.36 mg after 1 h 50 min of reaction). Note that this total amount of carbon, which can be hydrogenated by TPH, represents only about 5% after 25 min and 2% after 1 h 50 min of the amount of carbon, which can be oxidised by TPO (3.1 mg after 25 min and 16.2 mg after 1 h 50 min of reaction). Additional TPO tests directly performed after each TPH experiment confirm that a large part of the carbon deposits which accumulate on the catalyst is non-reactive towards hydrogen.

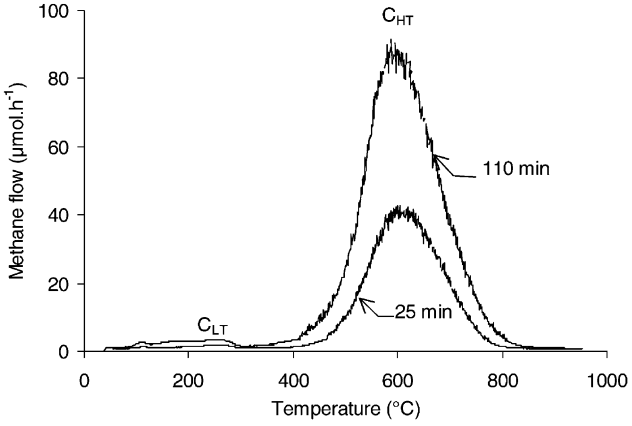

Fig. 2. Temperature Programmed Hydrogenation after 25 and 110 min of reaction.

Fig. 3(a) and (b) show the TEM images of the catalyst before and after reaction at deactivating conditions ($T = 500\ ^\circ C$, $H_2O/EtOH = 3.7$ and $O_2/EtOH = 0$) for 20 h, respectively. Before reaction, the metal particles are homogeneously dispersed (Fig. 3a) with an average size of 4 nm that corresponds to a dispersion of 28–30%. Carbon deposits are presented as multilayer 'shells' of graphitic nature that encapsulate metal particles as shows Fig. 3b. After reaction, a light particle sintering is observed, corresponding to an average metal dispersion to about 25%. Some bigger faceted particles appeared (Fig. 3b) always coexisting with the small, spherical initial particles.

3.3. Effect of the $H_2O/EtOH$ molar ratio

Among the specifications required for an on-board reformer, the capacity and weight of the fuel tank have a large influence on the car performances [26]. The objective was to minimise the tank weight and volume while maintaining a hydrogen production for a 500 km range. The temperature of 600 °C is chosen for testing these parameters as above mentioned. At 600 °C the conversion of water does not exceed 50%, which permits to reduce the water concentration in the feed without changing too much the performances. The effect of the $H_2O/EtOH$ molar ratio on reforming performances at 600 °C is reported in Fig. 4.

Whatever, the amount of water initially introduced, ethanol is completely converted and no partial oxidation (POX) products (aldehyde, acid) are detected. By decreasing the $H_2O/EtOH$ molar ratio, the selectivity to methane and the carbon deposition on the catalyst only slightly increase (from 110 to 130 mg h^{-1} and g of catalyst), while the selectivity to hydrogen slightly decreases. Thus, the initial concentration of water can be greatly reduced before getting a significant detrimental effect on hydrogen selectivity. The most significant effect upon minimising water content is to decrease the CO_2/CO_x molar ratio (i.e. the increase of the CO production), as expected from the water gas shift (WGS) equilibrium displacement. In order to counterbalance this

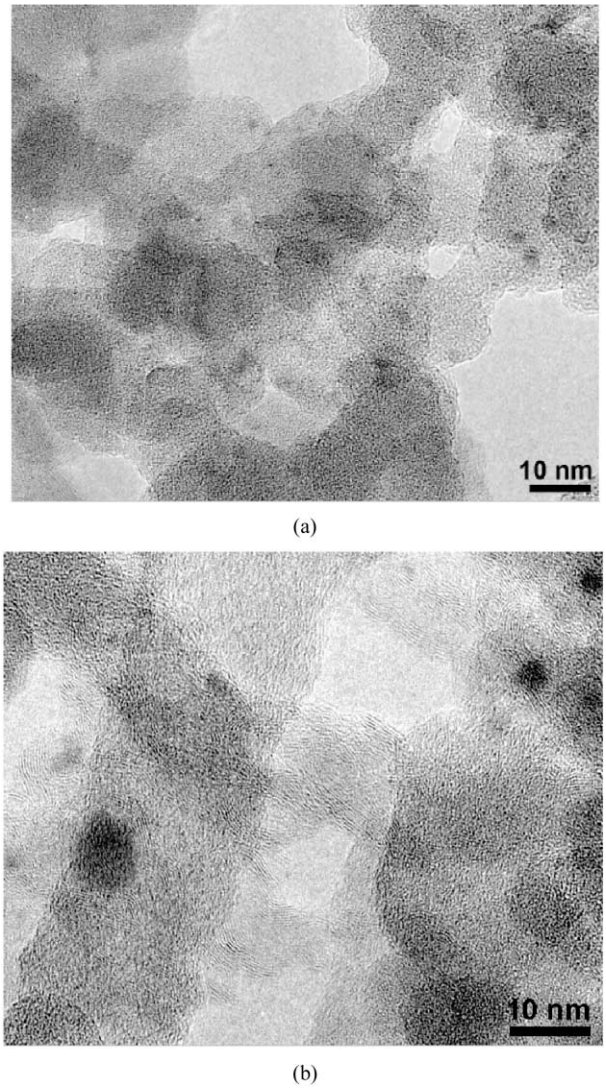

Fig. 3. TEM images of the catalyst: (a) before reaction; (b) after reaction ($T = 500\ ^\circ C$, $H_2O/EtOH = 3.7$ and $O_2/EtOH = 0$, $t_c = 0.9$ min kg mol^{-1} and reaction time = 20 h).

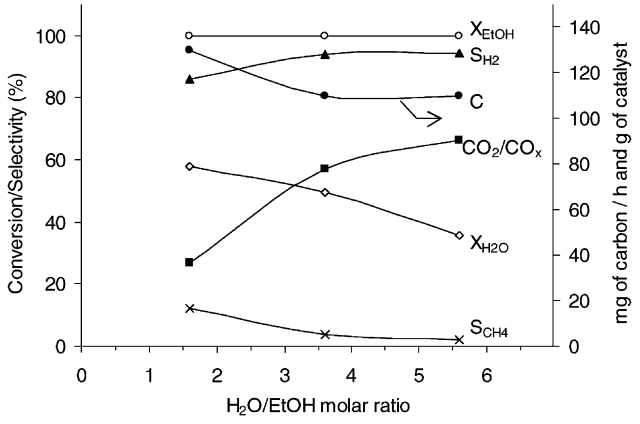

Fig. 4. Conversion of ethanol and water, selectivity to hydrogen and methane, CO_2/CO_x ratio and carbon deposition vs. $H_2O/EtOH$ molar ratio ($T = 600\ ^\circ C$, $O_2/EtOH = 0$ and $t_c = 0.9$ min kg mol^{-1}).

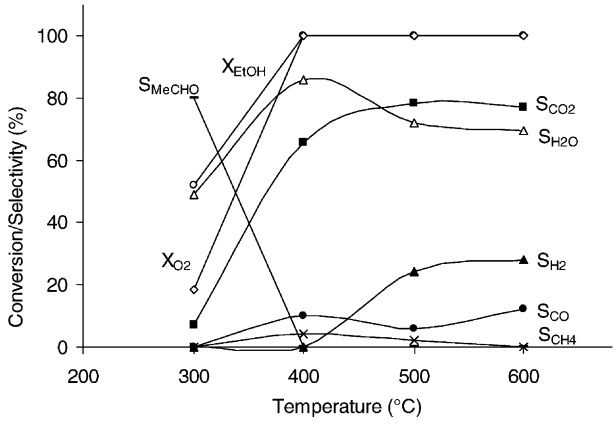

Fig. 5. Partial oxidation of ethanol. Conversion of ethanol and oxygen and product selectivity vs. temperature (O_2/EtOH = 1.55, H_2O/EtOH = 0 and t_c = 0.9 min kg mol^{-1}).

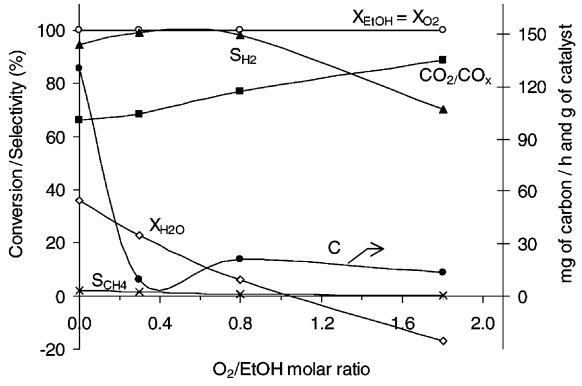

Fig. 6. Conversion of ethanol and water, selectivity to hydrogen and methane, CO_2/CO_x ratio, and carbon deposition vs. O_2/EtOH molar ratio (T = 600 °C, H_2O/EtOH = 5.6 and t_c = 0.9 min kg mol^{-1}).

negative effect, another oxidising source (O_2 or air) has to be introduced in the feed gas.

3.4. Reaction in the presence of oxygen

3.4.1. Partial oxidation of ethanol

In the absence of water and in the presence of oxygen, ethanol is to partially oxidised according to the reaction: $C_2H_5OH + (3/2)O_2 = 3H_2 + 2CO_2$. Note that only the POX of methanol was studied up to now, for which catalysts such as Cu/ZnO [27] or Pd/ZnO [28] have been tested.

To investigate ethanol POX, an oxygen/ethanol mixture (O_2/EtOH = 1.55) is admitted into the reactor to follow the influence of O_2 on the POX reaction at different temperatures (Fig. 5). At 300 °C the main product of the reaction is acetaldehyde. At 400 °C and above, the conversion of oxygen and ethanol is complete, whereas carbon dioxide and water are the main products. The hydrogen production and the selectivity to carbon monoxide remain low. Thus, even if the POX of ethanol cannot be envisioned as a direct route for hydrogen production, the results show that adding oxygen to the feed gas improves the CO_2/CO_x ratio.

3.4.2. Steam reforming of ethanol in the presence of oxygen

From the above results, the steam reforming of ethanol is performed in the presence of oxygen in order to reduce the carbon monoxide selectivity. The effects of oxygen addition for a given H_2O/EtOH molar ratio are presented in Fig. 6.

Over the whole tested O_2/EtOH range, ethanol and oxygen are completely converted. The conversion of water drops in the presence of O_2, being negative for O_2/EtOH ratio above 1.0. This indeed derives from the side production of water by hydrogen oxidation. In the corresponding O_2/EtOH range, the hydrogen selectivity is calculated only with respect to the consumed ethanol. It is interesting to note that at low O_2/EtOH ratio (below 0.8), the selectivity to hydrogen is unexpectedly slightly increased, while the CO selectivity is decreased, as expected. In addition, a dramatic effect on carbon deposition is observed as soon as oxygen is added to the feed. Thus, adding a small amount of oxygen to the feed (corresponding to an O_2/EtOH molar ratio equal to 0.8 for example) keeps the hydrogen selectivity close to 100%, while leading to a CO_2/CO_x ratio multiplied by 1.2, a carbon deposition divided by more than a factor of five and practically no methane production.

3.4.3. Effect of the molar ratio H_2O/EtOH in the presence of oxygen

Decreasing the water content in the feed gas was shown to markedly reduce the CO_2/CO_x ratio (Fig. 4). Addition of oxygen is expected to compensate this detrimental effect, while keeping a high selectivity to hydrogen and a low formation of carbon on the catalyst.

The combined effects of H_2O/EtOH molar ratio and O_2 addition are presented in Table 1. The introduction of low

Table 1
Effects of the H_2O/EtOH and O_2/EtOH ratios on product selectivity[a]

T = 600 °C	S_{H_2} (%)	CO_2/CO_x (%)	Carbon deposition (mg h^{-1} and g of catalyst)	S_{CH_4} (%)
H_2O/EtOH ratio = 3.7, without addition of O_2	94.2	54.3	110	3.9
H_2O/EtOH ratio = 1.6, without addition of O_2	85.9	27	130	12.1
H_2O/EtOH ratio = 1.6, low addition of O_2: O_2/EtOH ratio = 0.5	92.5	42.7	48	4.5

[a] Ni-Cu/SiO_2 (total metal loading = 4.34 wt.%), under He dilution conditions.

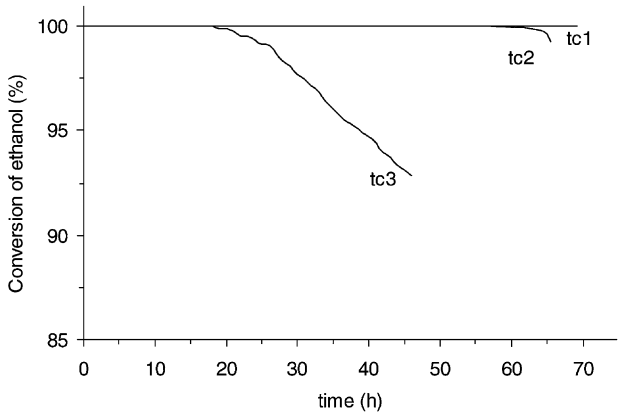

Fig. 7. Influence of the contact time on the conversion of ethanol ($t_{c1} = 1.33$, $t_{c2} = 0.65$ and $t_{c3} = 0.41$ min kg mol^{-1}) ($T = 600$ °C, H_2O/EtOH = 1.55 and O_2/EtOH = 0.5).

amounts of oxygen (O_2/EtOH = 0.5) both restores practically S_{H_2} to values obtained with twice the amount of added water and maintains the CO_2/CO_x ratio to an acceptable level in sight of further downstream shift steps. It is therefore quite feasible to reduce the amount of water in the feed gas and hence to reduce the capacity of the tank while keeping satisfying performances and markedly limiting the carbon formation and therefore catalyst deactivation.

3.5. Influence of contact time

In order to reduce the reformer reactor volume, the amount of catalyst has to be minimised, which can be achieved by reducing the contact time. The influence of contact time on the catalyst lifetime and on the product selectivities is illustrated in Figs. 7 and 8, respectively. When the amount of catalyst is decreased ($t_c \searrow$), the period of complete ethanol conversion, d, which gives an evaluation of the catalyst lifetime, is progressively decreased (Fig. 7): $d > 70$ h for $t_c = 1.33$ min kg mol^{-1}, $d = 60$ h for $t_c = 0.65$ min kg mol^{-1} and $d = 20$ h for $t_c = 0.41$ min kg mol^{-1}. In addition, it can be noted that the ethanol conversion decreases linearly for $t > d$. The H_2 and CH_4 selectivity, the CO_2/CO_x ratio and the H_2O conversion presented in Fig. 8 are average values calculated during the period of complete ethanol conversion for each contact time. No change in these parameters is observed over the contact time range studied. However, as soon as ethanol is no longer completely converted ($t > d$), C_2-species (such as acetaldehyde) are detected in the effluents.

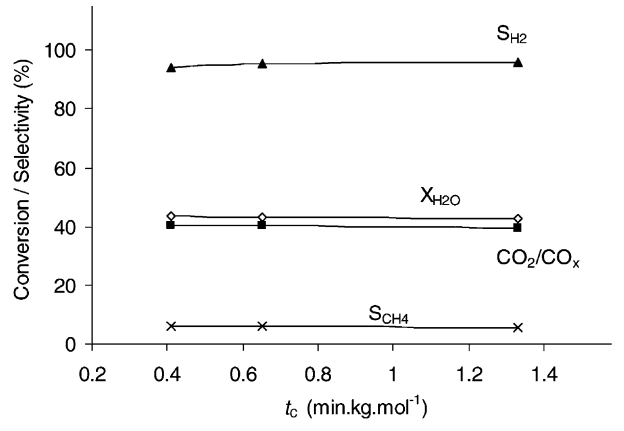

Fig. 8. Influence of the contact time on the conversion of water, on the selectivity to hydrogen and methane and on the CO_2/CO_x ratio ($T = 600$ °C, H_2O/EtOH = 1.55 and O_2/EtOH = 0.5).

4. Discussion

4.1. Nature of carbon deposits under reforming conditions, catalyst ageing

As no water is formed during TPO and TPH experiments carried out after long term reforming runs, it can be deduced that most of the carbonaceous species accumulating under reforming conditions are pure carbon (and not CO_x or CH_x adspecies). The small amount of carbon that is hydrogenated at low temperatures (C_{LT}) during TPH (also noted C_α as proposed by several authors [29,30] who established a recognised nomenclature of the various forms of carbon deposits) is most likely a surface nickel carbide Ni_3C, since a rough evaluation of the $Ni_{surface}/C_{LT}$ atomic ratio (calculated from the dispersion of nickel, determined from TEM measurement as mentioned later, and the integrated amount of low temperature carbon) gives values close to 3. Additional measurements of $Ni_{surface}/C_{LT}$ versus time are in progress to confirm this hypothesis, in good keeping with the surface carbidization reported during hydrocarbon reforming on nickel based catalyst, whatever the nature of the reformed hydrocarbon [31,32]. Note that this form of highly reactive carbon is generally directly related to the reforming process and cannot be considered as an ageing agent.

Regardless of the reaction time, the main carbon deposited on the catalyst (C_{HT}) is found very little reactive, since it can be only partially hydrogenated even at 900 °C and only reacts completely with oxygen during TPO experiments. Such a low reactivity and the observation that the deposited amount increases almost proportionally with reforming time (260 μmole after 25 min and 1320 μmole after 110 min of reaction) suggest that this kind of carbon is graphitic and accumulates around the metal particles, as reported for methane reforming over similar catalysts [31]. Electron microscopy measurements have confirmed this pattern of carbon accumulation (Fig. 3a and b), stressing its both crystallized and amorphous polymorphic structure.

The poisoning effect of this encapsulating carbon on the reforming reaction is obvious, since the catalyst is fully regenerated after burning that carbon and reducing again the catalyst. In addition, the catalyst poisoning most likely proceeds as a moving front along the catalyst bed as strongly suggested by the linear deactivation as depicted in Fig. 7.

The stability of the selectivities when the ethanol conversion remains complete agrees well with the picture of a catalyst bed progressively, but not selectively, poisoned by carbon. However, the appearance of C_2-compounds (as acetaldehyde) when the ethanol conversion starts to decline confirms that acetaldehyde may be an intermediate product of ethanol oxyreforming.

From the above analysis of contact time effects showing that the selectivity is stable till the ethanol conversion starts to decline, it can be concluded that the size of the steam reforming reactor will therefore result from a compromise between the technical constraints to reduce its capacity and the optimization of the catalyst lifetime.

4.2. Kinetic scheme

The kinetic scheme has to be discussed as a function of the temperature domain.

$C_2H_5OH = CH_3CHO + H_2$ (reaction 1)

$C_2H_5OH = CH_4 + CO + H_2$ (reaction 2)

$C_2H_5OH = 2C + H_2O + 2H_2$ (reaction 3)

$CH_4 + H_2O = CO + 3H_2$ (reaction 4)

$CO + H_2O = CO_2 + H_2$ (reaction 5)

$H_2 + \frac{1}{2}O_2 = H_2O$ (reaction 6)

$CO + \frac{1}{2}O_2 = CO_2$ (reaction 7)

$CH_4 + 2O_2 = CO_2 + 2H_2O$ (reaction 8)

$C_2H_5OH + \frac{1}{2}O_2 = CH_3CHO + H_2O$ (reaction 9)

$C_2H_5OH + 3O_2 = 2CO_2 + 3H_2O$ (reaction 10)

$C + O_2 = CO_2$ (reaction 11)

At 300 °C and in the absence of oxygen, the acetaldehyde formation results from ethanol dehydrogenation [17] (reaction 1). However, by observing in Fig. 1 that $S_{CH_4} = S_{CO}$ at 300 °C, it can be deduced that most of the ethanol is cracked into methane and carbon monoxide [15,16] following reaction 2. Since no toxic carbon deposition is usually observed from CH_4 or CO/H_2 at low temperature [32], the accumulating carbon (distinct from the active surface carbide) has to be directly formed from ethanol, possibly via C_2-compound and according to the overall reaction 3. In order to check the validity of this scheme, the observed hydrogen selectivity can be calculated. According to the proposed reactions: $F_{H_2} = F_{MeCHO} + F_{CO} + F_C$, so $S_{H_2} = F_{H_2}/3F_{EtOH\,in}$ (because $X_{EtOH} = 100\%$) $= [F_{MeCHO} + F_{CO} + F_C]/3F_{EtOH\,in} = (1/3)S_{MeCHO} + (2/3)S_{CO} + (2/3)S_C = 38.8\%$. Within the experimental errors, the calculated value and the experimental value (41.7%) are practically similar. Similarly and according to this scheme: $F_{H_2O\,in} - F_{H_2O\,out} = -(1/2)F_C$, so $X_{H_2O} = [F_{H_2O\,in} - F_{H_2O\,out}]/F_{H_2O\,in} = [-(1/2)F_C]/3.7F_{EtOH\,in} = -(1/3.7)S_C = -4.1\%$, in good agreement with the experimental $X_{H_2O} = -3.8\%$.

At 400 °C the decomposition of acetaldehyde is complete, as expected from the thermal stability of that molecule [33,34]. The effluent gas composition is then controlled by the methane steam reforming (reaction 4, $\Delta H > 200\ kJ\ mol^{-1}$) and by the WGS (reaction 5, $\Delta H \approx -40\ kJ\ mol^{-1}$) equilibria. Thus, the thermodynamic equilibria of the two latter reactions (Fig. 9) explain the observed trends in selectivity changes in Fig. 1 when the temperature increases, water and methane are consumed and the hydrogen selectivity is improved.

At 600 °C the WGS equilibrium tends to be totally displaced and the reverse WGS starts to control the gas composition (Fig. 9). In addition, when the amount of water is severely decreased by decreasing the molar ratio H_2O/EtOH in the feed, both the reverse methane steam reforming

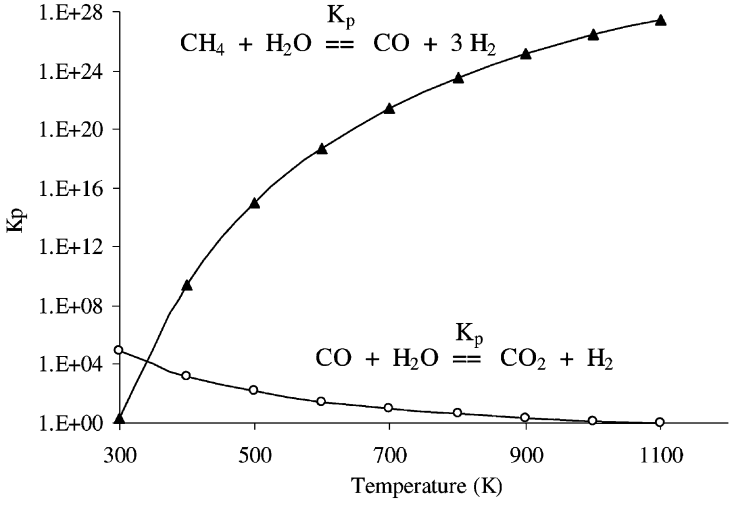

Fig. 9. Equilibrium constants of the methane steam reforming and water gas shift reactions vs. temperature. K_p is determined from Van't Hoff relation.

and WGS are favored, which improves the CH_4 selectivity at the expenses of the H_2 selectivity and greatly reduces the CO_2/CO_x ratio.

4.2.1. Role of oxygen

The presence of oxygen in the feed gas favors oxidation reactions (reactions 6–8). In addition, when the O_2 concentration becomes important at low temperature (O_2/EtOH = 1.55 and H_2O/EtOH = 0), ethanol can also be oxidised following reaction 9, which explains the high selectivity to water and acetaldehyde at 300 °C (Fig. 5). At higher temperatures the main reaction induced by oxygen addition is ethanol combustion (reaction 10). In the presence of water (H_2O/EtOH = 5.6) oxidation reactions explain also the conversions and selectivities obtained in Fig. 6. When the O_2/EtOH ratio is increased, methane and carbon monoxide are oxidised ($S_{CH_4} \searrow$ and $CO_2/CO_x \nearrow$). In the same way hydrogen is also oxidised into water, which explains the lower H_2 selectivity and a negative value for water conversion ($F_{H_2O\,in} < F_{H_2O\,out}$). Fortunately, the selectivity to hydrogen does not decrease upon introducing a small amount of oxygen (O_2/EtOH < 0.8) and it is even slightly improved. This can be explained by the reduction of the water conversion, that is directly coupled to the H_2 selectivity: $S_{H_2} = F_{H_2}/[3(F_{EtOH\,in} - F_{EtOH\,out}) + (F_{H_2O\,in} - F_{H_2O\,out})] = kF_{H_2}/[K + X_{H_2O}]$, where k and K are constants. At 600 °C the presence of oxygen greatly reduces the carbon formation, because the carbon is oxidised at 580 °C under an oxygen stream (reaction 11 according to the results of TPO).

4.3. Optimisation of the operating conditions

The optimisation of the experimental conditions aims mainly at maximizing the H_2 yield while limiting the CO formation which represents a severe SPFC anode poison. In this way, running the reforming reaction at 600 °C seems to be satisfactory, since it induces an important H_2 production while maintaining a sufficiently high CO_2/CO_x ratio for the further downstream shift process.

Concerning the mass of catalyst used (contact time), it has been shown that it can be reduced without significant changes in the selectivity to reaction products (see Fig. 8), but it reduces the lifetime of the catalyst (Fig. 7). Therefore, a good compromise between reactor volume and catalyst life-time must be reached.

In the present study, the ethanol steam reforming is proposed as a process step allowing electricity to be produced from a liquid fuel via a fuel cell. The criteria for optimisation of the experimental parameters must therefore take into account the technological constraints imposed by this system: (i) the production of hydrogen must be sufficiently high to supply a SPFC powering system; (ii) the H_2O/EtOH ratio must be appropriate for a tank of reasonable capacity and weight; (iii) the carbon deposition on the catalyst must be limited in order to improve the system lifetime; (iv) the CO concentration must be reduced as much as possible in sight of the further downstream CO shift and selective oxidation, considering the low tolerance to CO of the fuel cell anode and finally; (v) the above defined contact time (i.e. the catalyst loading) must keep the reformer within acceptable dimensions. The experimental conditions under helium atmosphere that seem to be the best answer to fit these requirements are a reaction temperature close to 600 °C, a H_2O/EtOH molar ratio equal to 1.6, a limited introduction of oxygen (molar ratio of O_2/EtOH = 0.5) and a contact time close to 1 min kg mol^{-1}.

As indicated in the introduction, additional experiments were done under closer on-board reforming conditions, i.e. using ethanol, water and air as reactant and the process has been patented [25]. The use of air fixes the ratio O_2/inert and therefore the partial pressures of the reactants and products are higher leading to changes in the reaction rates and in the selectivities. The optimised experimental conditions involve a reforming temperature close to 700 °C, a molar ratio of H_2O/EtOH equal to 1.6, a molar ratio of O_2/EtOH equal to 0.68 and a contact time close to 0.2 min kg mol^{-1}. Since, the commercial development of oxidative reforming of ethanol requires a good stability of the catalyst, the latter was tested for 140 h at the optimized operating conditions. The catalyst exhibited a constant selectivity to the reaction products and the ethanol was totally converted during this time. The outlet composition presents a percentage of hydrogen of 33.0%, lower concentrations of CO and CO_2 (12.9 and 9.2%, respectively) and a much smaller concentration of methane (1.4%).

5. Conclusion

High temperatures and introduction of oxygen in the feed gas are shown to favor the production of hydrogen, while limiting the formation of methane and carbon deposition. However, even if the addition of O_2 reduces the carbon monoxide concentration, the latter remains much higher than the tolerance threshold of the fuel cell. A further CO abatement (HT and LT WGS followed by a selective oxidation of CO) has to be considered at the reformer outlet. After different tests under on-board-like conditions, an estimate of the global process has been patented [25]. This study has also allowed us to point out some kinetic trends and to propose an overall reaction scheme as a function of the temperature domain. A more detailed mechanistic study is in progress.

References

[1] G.G. Harding, J. Power Sources 78 (1999) 193–198.
[2] M. Cenek, J. Kazelle, J. Power Sources 80 (1999) 301.
[3] G.J.K. Acres, J.C. Frost, G.A. Hards, R.J. Potter, T.R. Ralph, D. Thompsett, G.T. Burstein, G.J. Hutchings, Catal. Today 38 (1997) 393–400.
[4] C. Sishtla, G. Koncar, R. Platon, S. Gamburzev, A.J. Appleby, O.A. Velev, J. Power Sources 71 (1998) 249–255.

[5] N. Edward, S.R. Ellis, J.C. Frost, S.E. Golunski, A.N.J. Vankeulen, N.G. Lindewald, J.G. Reinkingh, J. Power Sources 71 (1998) 123.
[6] B. Emonts, J.B. Hansen, S.L. Jorgensen, B. Höhlein, R. Peters, J. Power Sources 71 (1998) 288.
[7] S. Kawatsu, J. Power Sources 71 (1998) 150–155.
[8] F. Panik, J. Power Sources 71 (1998) 36–38.
[9] G. Maggio, S. Freni, S. Cavallaro, J. Power Sources 74 (1998) 17.
[10] E.Y. Garcia, M.A. Laborde, Int. J. Hydrogen Energy 16 (1991) 307–312.
[11] K. Vasudeva, N. Mitra, P. Umasankar, S.C. Dhingra, Int. J. Hydrogen Energy 21 (1996) 13–18.
[12] S. Freni, G. Maggio, S. Cavallaro, J. Power Sources 62 (1996) 67–73.
[13] I. Fishtik, A. Alexander, R. Datta, D. Geana, Int. J. Hydrogen Energy 25 (2000) 31–45.
[14] T. Ioannides, J. Power Sources 92 (1–2) (2001) 17–25.
[15] M. Morita, A. Sato, Y. Matsuda, Nippon Kagaku Kaishi, (1993) 164–169.
[16] C.A. Luengo, G. Ciampi, M.O. Cenzig, C. Steckelberg, M.A. Laborde, Int. J. Hydrogen Energy 17 (1992) 677–681.
[17] N. Iwasa, N. Takezawa, Bull. Chem. Soc. Jpn. 64 (1991) 2619–2623.
[18] S. Cavallaro, S. Freni, Int. J. Hydrogen Energy 21 (1996) 465–469.
[19] F. Haga, T. Nakajima, K. Yamashita, S. Mishima, S. Suzuki, Nippon Kagaku Kaishi 1 (1997) 33–36.
[20] F. Haga, T. Nakajima, K. Yamashita, S. Mishima, Nippon Kagaku Kaishi 11 (1997) 758–762.
[21] F. Haga, T. Nakajima, K. Yamashita, S. Mishima, Catal. Lett. 48 (1997) 223–227.
[22] F. Haga, T. Nakajima, K. Yamashita, S. Mishima, React. Kinet. Catal. Lett. 63 (1998) 253–259.
[23] F.J. Mariño, E.G. Cerrella, S. Duhalde, M. Jobbagy, M.A. Laborde, Int. J. Hydrogen Energy 23 (12) (1998) 1095–1101.
[24] S. Freni, J. Power Sources 94 (1) (2001) 14–19.
[25] V. Graziani-Klouz, C. Marquez-Alvarez, C. Mirodatos, F. Michalak, J.P. Lisse, French Patent No. 99.08083.
[26] K. Yamane, S. Furuhama, Int. J. Hydrogen Energy 23 (1998) 825–831.
[27] L. Alejo, R. Lago, M.A. Pena, J.L.G. Fierro, Appl. Catal. A-General 162 (1997) 281–297.
[28] M.L. Cubeiro, J.L.G. Fierro, Appl. Catal. A-General 168 (1998) 307–322.
[29] P. Winslow, A.T. Bell, J. Catal. 86 (1984) 158.
[30] C.H. Bartholomew, Catal. Rev. Sci. Eng. 24 (1982) 67.
[31] V.C.H. Kroll, H.M. Swaan, C. Mirodatos, J. Catal. 161 (1996) 409.
[32] M. Agnelli, H.M. Swaan, C. Marquez-Alvarez, G.A. Martin, C. Mirodatos, J. Catal. 177 (1998) 105–112.
[33] J. G. Highfield, F. Geiger, E. Uenala, V. Shklover, T. H. Schucan, in: Proceedings of the 10th International Symposium on Alcohol Fuels, Vol. 1, 1993, p. 238.
[34] J.G. Highfield, F. Geiger, E. Uenala, T.H. Schucan, Editors: D.L. Block, T.N. Veziroglu, Hydrogen Energy Prog. X, Proc. World Hydrogen Energy Conf. 10th (1994), 2, 1039–1049. Publisher: Fla. Sol. Energy Cent.